

# An AIEE Active Anthracene-Based Nanoprobe for Zn<sup>2+</sup> and Tyrosine Detection Validated by Bioimaging Studies

Muthaiah Shellaiah,<sup>1</sup> Natesan Thirumalaivasan,<sup>1</sup> Basheer Aazaad,<sup>1</sup> Kamlesh Awasthi,<sup>1,2</sup> Kien-Wen Sun,<sup>1\*</sup> Shu-Pao Wu,<sup>1</sup> Ming-Chang Lin,<sup>1</sup> Nobuhiro Ohta<sup>1,2</sup>

<sup>1</sup>Department of Applied Chemistry, National Yang Ming Chiao Tung University, Hsinchu 300 and Taiwan

<sup>2</sup>Center for Emergent Functional Matter Science, National Yang Ming Chiao Tung University, Hsinchu 300, Taiwan

\* Correspondence: Prof. Kien Wen Sun, Department of Applied Chemistry, National Yang Ming Chiao Tung University, Hsinchu 300, Taiwan, R.O.C. Tel: +886-(03)571-2121 ext. 56581 E-mail: [kwsun@nycu.edu.tw](mailto:kwsun@nycu.edu.tw)

## Table of contents

General information and procedure for data collection	(Page: S1-S2)
<sup>1</sup> H, <sup>13</sup> C-NMR and HR-mass data of AT2	(Page: S3-S4)
UV/PL, TRPL changes of AT2 to AIEE and sensors; pH effect on sensors	(Page: S5-S10)
Job's plots, HR-mass spectra, association-constant evaluation for sensor complexes	(Page: S11-S14)
SEM, TEM, AFM and DLS data related to AIEE and sensors	(Page: S15-S19)
H-NMR titrations DFT optimizations on AIEE and Sensory complexes	(Page: S20-S23)
MTT assay and cell imaging related to AIEE and Zn <sup>2+</sup> photostability	(Page: S24-S25)
Comparative tables for Zn <sup>2+</sup> and Tyrosine sensors	(Page: S26-S27)

## General Information

Anthracene-9-carboxaldehyde and 4-Amino-5-phenyl-4H-1,2,4-triazole-3-thiol were purchased from Sigma-Aldrich (Taiwan Merck Co., Ltd, Taipei, Taiwan) and AT2 (4-(anthracen-9-ylmethylene)amino)-5-phenyl-4H-1,2,4-triazole-3-thiol) was synthesized according to the literatures [3, 15]. Agilent-NMR400 and Bruker 300 MHz (<sup>1</sup>H: 400 MHz; <sup>13</sup>C: 75 MHz) spectrometer were used to collect the <sup>1</sup>H and <sup>13</sup>C NMR spectral data, respectively. Deuterated dimethyl sulfoxide (DMSO-d<sub>6</sub>) and deuterated ethanol (C<sub>2</sub>D<sub>6</sub>O) were used for <sup>1</sup>H NMR samples preparation and titrations. The chemical shifts (δ) and coupling constants (J) were designated in ppm and in Hz, consistently. Impact HD Q-TOF mass spectrometer (Bruker, Germany) was engaged for Mass analysis. Agilent 8453 UV-Visible spectrometer and Hitachi F-4500 spectrometer were employed in UV/PL spectroscopic investigations, separately. A home-made time-correlated single photon-counting (TCSPC) spectrometer was engaged in time-resolved photoluminescence (TRPL) spectral studies [53]. pH [1–14] buffers were freshly prepared for pH-effect studies [54, 55]. Cellular and Zebra-fish images were collected from multiphoton and confocal microscope system, Leica, Germany, TCS-SP5-X AOBs.

## Stock solutions for sensory inquiries

From 100 mM, 10 mM, 2 mM and 1 mM stock solutions (in DMSO; mM = millimole), the AT2-probe at 50 μM (μM = micromole) concentration in absolute ethanol (99.9%) was prepared for AIEE and sensor studies. From respective chloro or acetate compounds, metal ions (Mg<sup>2+</sup>, Mn<sup>2+</sup>, Ni<sup>2+</sup>, Co<sup>2+</sup>, Pb<sup>2+</sup>, Al<sup>3+</sup>, Cs<sup>+</sup>, Na<sup>+</sup>, K<sup>+</sup>, Cd<sup>2+</sup>, Ca<sup>2+</sup>, Zn<sup>2+</sup>, Hg<sup>2+</sup>, Cu<sup>2+</sup>, Ba<sup>2+</sup>, Sn<sup>2+</sup>, Fe<sup>2+</sup>, Cr<sup>3+</sup>, Y<sup>3+</sup>, Ga<sup>3+</sup>, Pd<sup>2+</sup> and Fe<sup>3+</sup>) were prepared at 10 mM concentration in deionized (DI) water. Potassium-dichromate (K<sub>2</sub>Cr<sub>2</sub>O<sub>7</sub>; 10 mM) was used as Cr<sup>6+</sup> ions source. Likewise, amino acids [Ala: Alanine; Ser: Serine; DA: Dopamine; Met: Methionine; Glu-acid: Glutamic acid; His: Histidine; Glu: Glucose; Thr: Threonine; Tyr: Tyrosine; AA: Ascorbic acid; Lys: Lysine; Phe-Ala: Phenyl Alanine; Orn: Ornithine; Gly: Gly-

cine; Arg: Arginine; Cys: Cysteine; H-Cys: Homo-Cysteine; GSH: Glutathione; Try: Tryptophan; Pro: Proline; Leu: Leucine; GA: Glutamine] were prepared at 10 mM concentration in DI-water.

#### Procedure for AIEE and sensory studies [15]

**AIEE:** For 0-90%  $f_w$ , 5  $\mu\text{L}$  of **AT2** probe (from 10 mM stock solution) was taken in 10 separate vials and diluted with 995 to 95  $\mu\text{L}$  ethanol with a decreasing equal span of 100  $\mu\text{L}$ . To those vials 0-900  $\mu\text{L}$  of DI-water was added with increasing equal span of 100  $\mu\text{L}$ . For 97.5%  $f_w$ , 25  $\mu\text{L}$  of **AT2** probe (from 2 mM stock solution) was directly mixed with 975  $\mu\text{L}$  of DI water. Thereafter, all the AIEE samples were subjected to PL investigations; Note: the final concentration of **AT2** in all the bottles was maintained as 50  $\mu\text{M}$ .

**Zn<sup>2+</sup> sensors:** 5  $\mu\text{L}$  of **AT2** probe (from 10 mM stock solution) was added in to separate vials, diluted with 992.5  $\mu\text{L}$  ethanol and then mixed with 2.5  $\mu\text{L}$  of metal ions (from 10 mM stock solution. Above mixture subject to photographs (under UV-lamp ( $\lambda_{\text{ex}} = 365$  nm) and PL interrogations. For the interference study, the mixture contains "5  $\mu\text{L}$  of **AT2** probe (from 10 mM stock solution) + 985  $\mu\text{L}$  ethanol + 2.5  $\mu\text{L}$  of Zn<sup>2+</sup> (from 10 mM stock) + 7.5  $\mu\text{L}$  of competing metal ions" and subjected to PL investigations. Next, individual titrations contained "5  $\mu\text{L}$  of **AT2** probe (from 10 mM stock solution) + 992.5  $\mu\text{L}$  ethanol + 2.5  $\mu\text{L}$  of Zn<sup>2+</sup> (from 1-14 mM stock with an equal span of 1 mM)". For pH studies, use of pH buffer (20  $\mu\text{L}$ , 10 mM stock) was adjusted by altering ethanol volume.

**Tyrosine sensors:** To the solution containing "5  $\mu\text{L}$  of **AT2** probe (from 10 mM stock solution) + 990  $\mu\text{L}$  ethanol + 2.5  $\mu\text{L}$  of Zn<sup>2+</sup> (from 10 mM stock)", 2.5  $\mu\text{L}$  of aminoacids (from 10 mM stock) were added in separate vials and used in photographic and PL studies. During the interference studies, the above mixture was further altered by reducing ethanol volume to 982.5  $\mu\text{L}$  along with addition of 7.5  $\mu\text{L}$  of competing aminoacids. Individual titration mixture used 990  $\mu\text{L}$  ethanol by varying Tyrosine concentration (2.5  $\mu\text{L}$  from 1-14 mM stock with an equal span of 1 mM). Note: for all AIEE and sensory studies, final volume fixed as 1 mL.

#### NMR titrations and Mass interrogations [15]

20 mM of **AT2** (1 equiv. in DMSO- $d_6$ ) was titrated with 12 mM of Zn<sup>2+</sup> [0.6 equiv.; source Zinc(II) perchlorate in deuterated ethanol ( $\text{C}_2\text{D}_6\text{O}$ )]. Following two complexes were prepared for HR-Mass analysis; 1. 50 mM of **AT2** (in DMSO) + 25 mM of Zn<sup>2+</sup> ions [ $\text{Zn}(\text{OAc})_2$  in water]; 2. 50 mM of **AT2** (in DMSO) + 25 mM of Zn<sup>2+</sup> ions [ $\text{Zn}(\text{OAc})_2$  in water] + 25 mM of Tyrosine (in water). Above two mentioned complexes were stirred separately for 30 min at room temperature (RT), dried in hot air-oven at 120°C for 3 hours to remove the solvent and then subjected to mass analysis.

#### SEM and AFM imaging [15]

Over a well cleaned surface of Si-wafers (0.5  $\times$  0.5 cm), 20  $\mu\text{L}$  of samples were drop casted, dried in a hot air-oven at 60°C for 30 minutes (solvent evaporation) and then kept under vacuum for 3 hours to remove any solvent trace. To avoid moisture, the samples were placed in a vacuum sample chamber. SEM and AFM analysis of those samples were performed by Hitachi SU-8010 (Tokyo, Japan) and D3100 (EXW Charlotte, NC USA) instrumental set up, correspondingly.

#### TEM studies [15]

During TEM analysis, 5  $\mu\text{L}$  of samples were drop-casted over the surface of Cu/C grid (Carbon Type-B, 200 mesh, Cu; TED PELLA, INC., CA, USA). The sample-casted grids were dried at 50° C in a hot air oven for 30 minutes and then kept in a vacuum for 8 hours to remove the solvent. To avoid moisture, all samples (casted on Cu/C grids) were maintained in a vacuum chamber until the insertion into the TEM machine. Finally, Cu/C grids with samples were interrogated by JEOL-JEM-2100F (JEOL Ltd., Tokyo, Japan) at an operating accelerating voltage of 200 kV.

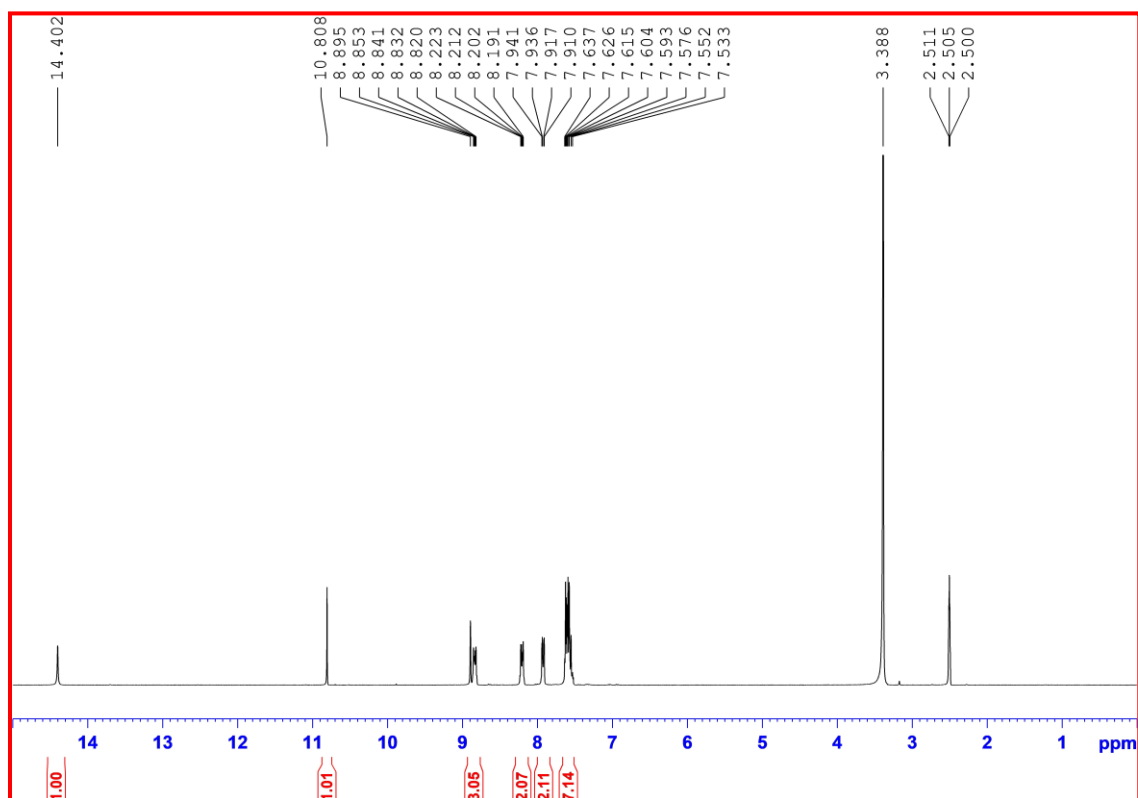


Figure S1. <sup>1</sup>H NMR spectrum of AT2.

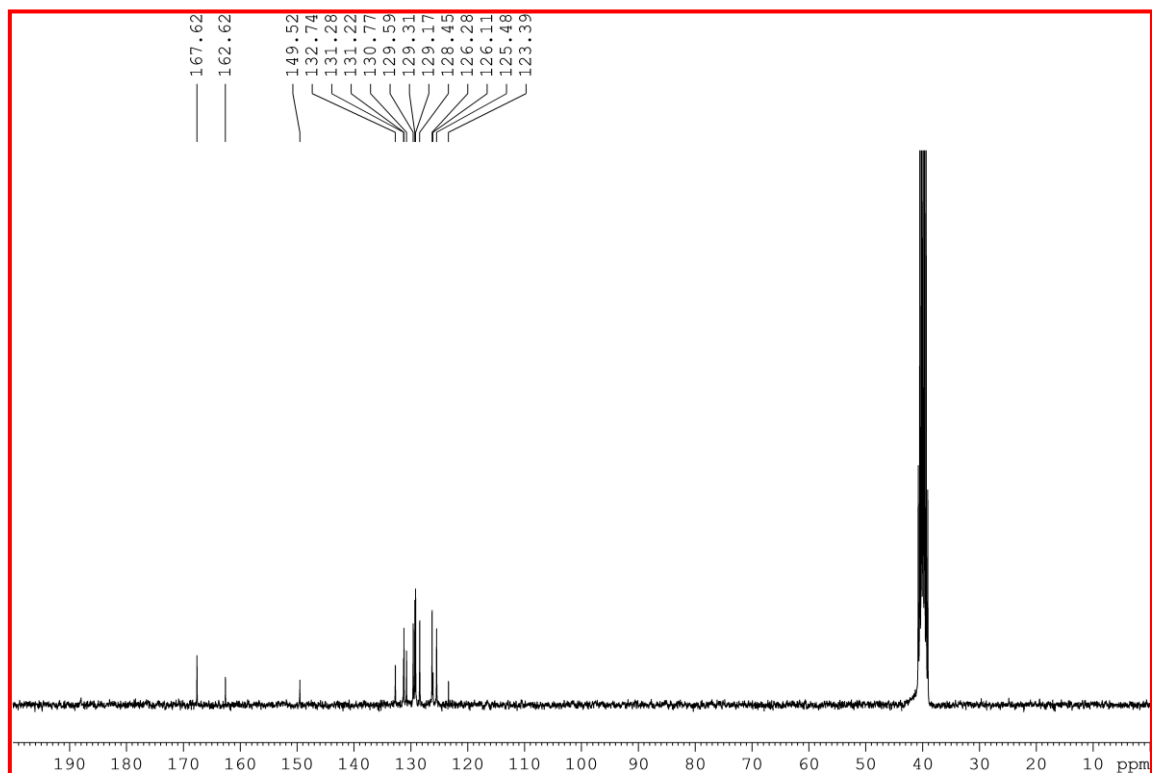


Figure S2. <sup>13</sup>C NMR spectrum of AT2.

## Display Report

### Analysis Info

Analysis Name D:\Data\nctu service\data\2019\20190730\2 AT2\_GC4\_01\_17643.d

Acquisition Date 7/30/2019 1:01:57 PM

Method Small molecule.m

Operator NCTU

Sample Name 2 AT2

Instrument impact HD 1819696.00164

Comment

### Acquisition Parameter

Source Type	ESI	Ion Polarity	Positive	Set Nebulizer	1.0 Bar
Focus	Active	Set Capillary	4500 V	Set Dry Heater	200 °C
Scan Begin	50 m/z	Set End Plate Offset	-500 V	Set Dry Gas	6.0 l/min
Scan End	1500 m/z	Set Charging Voltage	2000 V	Set Divert Valve	Waste
		Set Corona	0 nA	Set APCI Heater	0 °C

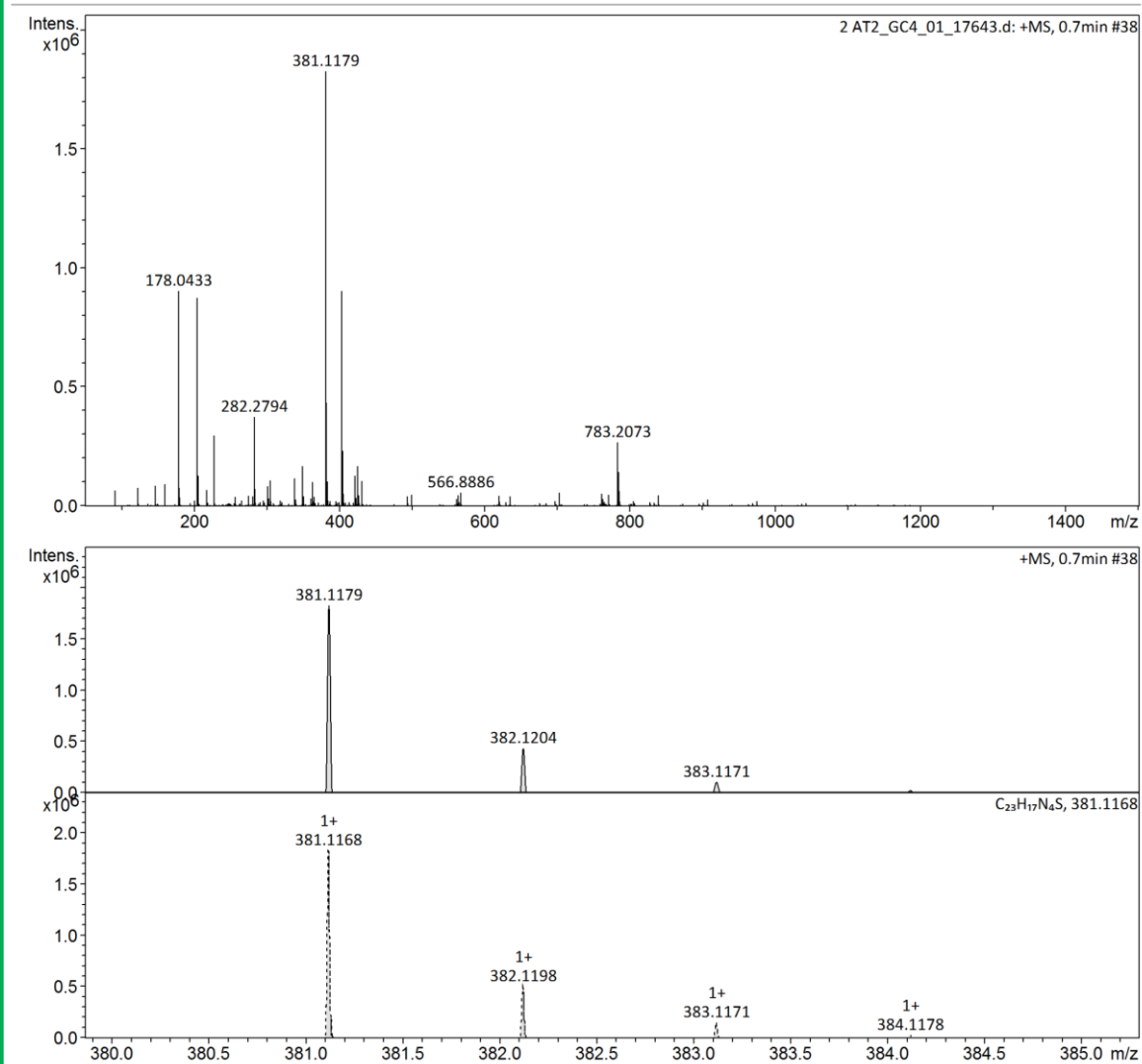


**Figure S3.** Mass spectrum of AT2 probe ( $M+H$ )<sup>+</sup>.

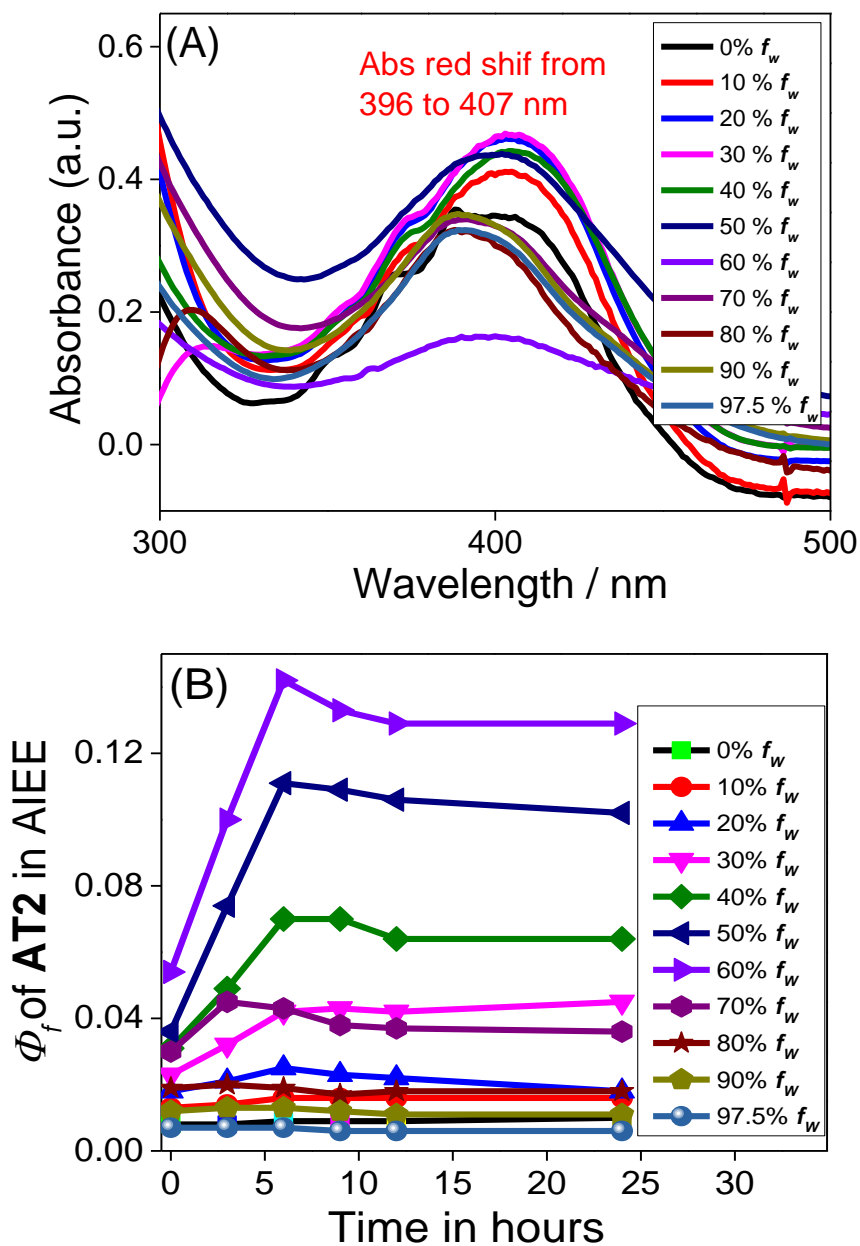


**Figure S4.** (A) UV-Vis spectra of **AT2** (50  $\mu\text{M}$  in ethanol) during the AIEE as a function of water fraction ( $f_w$ ); (B) Quantum yield changes of **AT2** (50  $\mu\text{M}$  in ethanol) with respect to water fraction variation from 0 to 97.5%  $f_w$  as a function of time (0-24 hours).

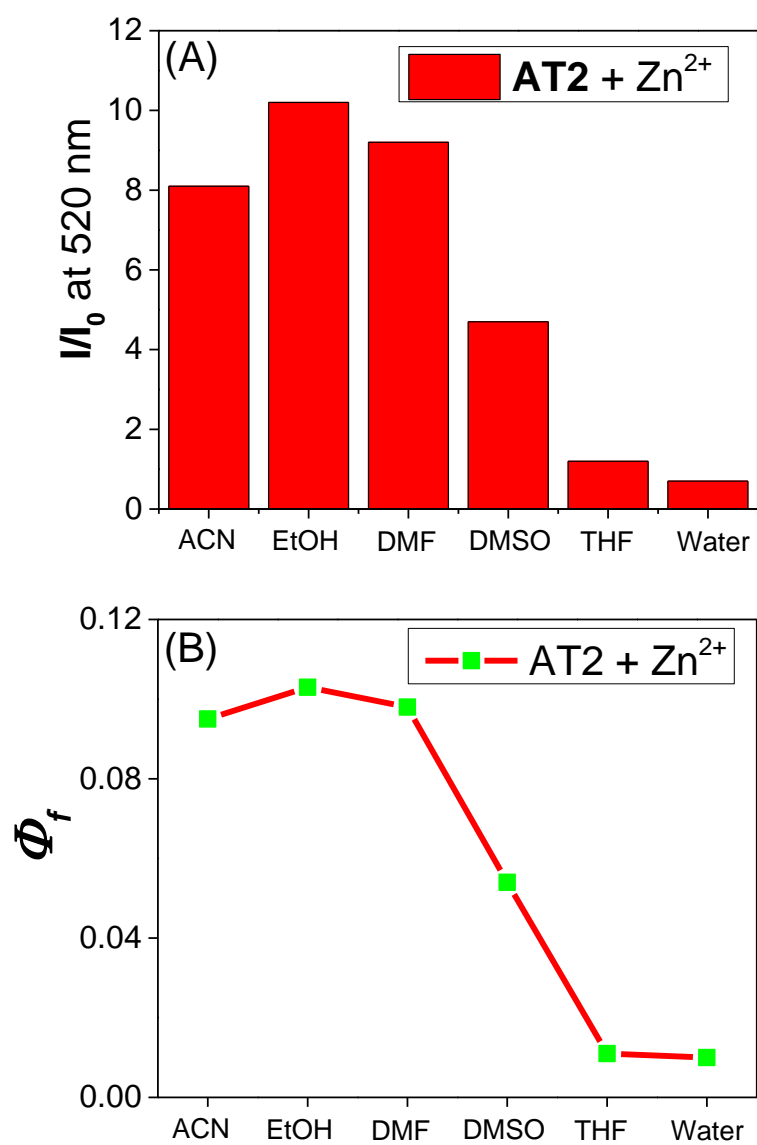


**Figure S5.** (A) Fold of enhancement during  $\text{AT2-Zn}^{2+}\text{-AT2}^*$  formation with respect to diverse solvent media; (B) Opted quantum yields for  $\text{AT2-Zn}^{2+}\text{-AT2}^*$  with respect to different solvent media.

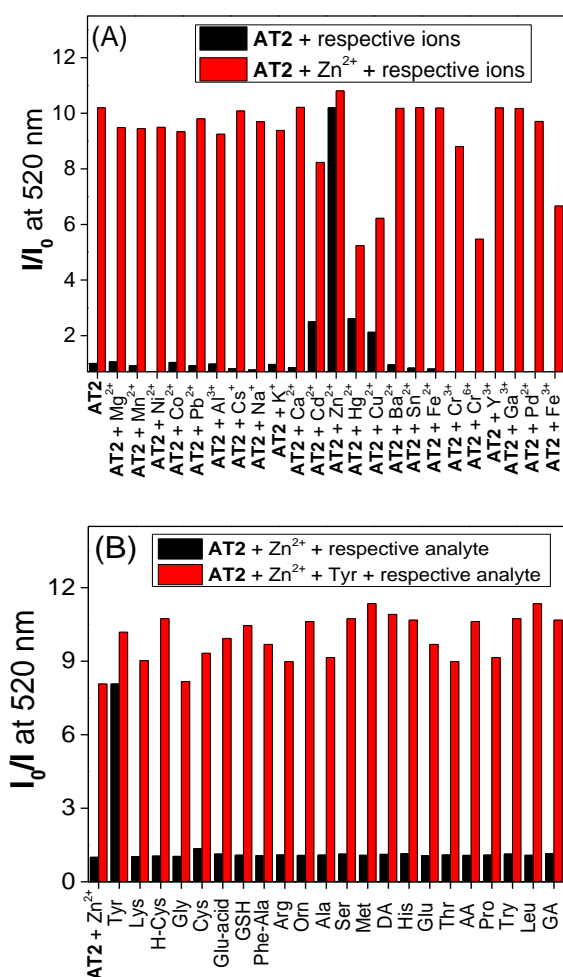


**Figure S6.** (A) Single and dual selectivity of **AT2** (50  $\mu\text{M}$  in ethanol) towards metal ions (Note: for single analyte investigations all metal ions were taken at 25  $\mu\text{M}$  concentration from 10 mM stock solution and for dual analyte studies  $\text{Zn}^{2+}$  and other ions were mixed at 1:3 ratio (25  $\mu\text{M}$  + 75  $\mu\text{M}$ ); (B) Single and dual selectivity of **AT2** +  $\text{Zn}^{2+}$  complex (50  $\mu\text{M}$  + 25  $\mu\text{M}$ ) towards amino acids (Note: for single analyte investigations all amino acids were taken at 25  $\mu\text{M}$  concentration from 10 mM stock solution and for dual analyte studies Tyrosine and other amino acids were mixed at 1:3 ratio (25  $\mu\text{M}$  + 75  $\mu\text{M}$ ) [Ala: Alanine; Cys: Cysteine; H-Cys: Homo-Cysteine; Met: Methionine; Glu-acid: Glutamic acid; His: Histidine; Tyr: Tyrosine; Glu: Glucose; Thr: Threonine; AA: Ascorbic acid; Lys: Lysine; Phe-Ala: Phenyl Alanine; Orn: Ornithine; Gly: Glycine; Arg: Arginine; .GSH: Glutathione; Ser: Serine; DA; Dopamine; Pro: Proline; Try: Tryptophan; Leu: Leucine; GA: Glutamine].

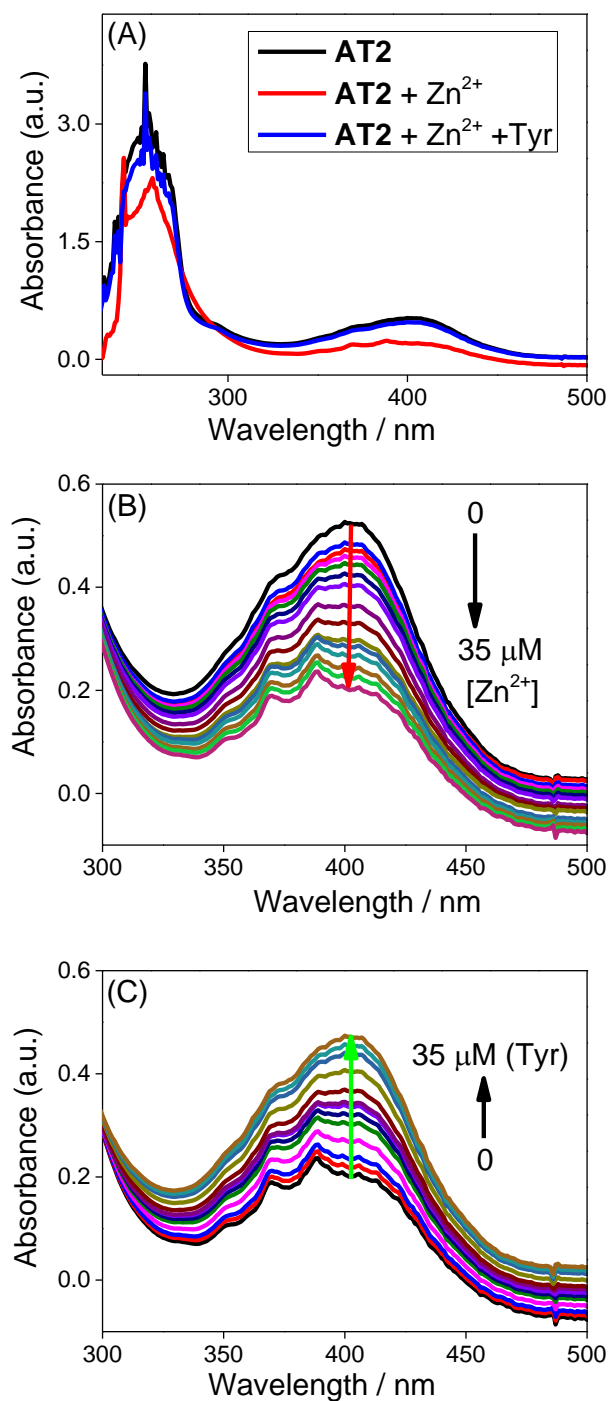


**Figure S7.** (A) UV-Vis spectra of **AT2** (50 μM in ethanol), **AT2** + Zn<sup>2+</sup> (50 μM in ethanol + 25 μM in H<sub>2</sub>O, correspondingly) and **AT2** + Zn<sup>2+</sup> + Tyr (50 μM in ethanol + 25 μM in H<sub>2</sub>O + 25 μM in H<sub>2</sub>O, individually); (B, C) UV-Vis titration of **AT2** and **AT2** + Zn<sup>2+</sup> complex with 0-35 μM of Zn<sup>2+</sup> and Tyrosine, respectively.



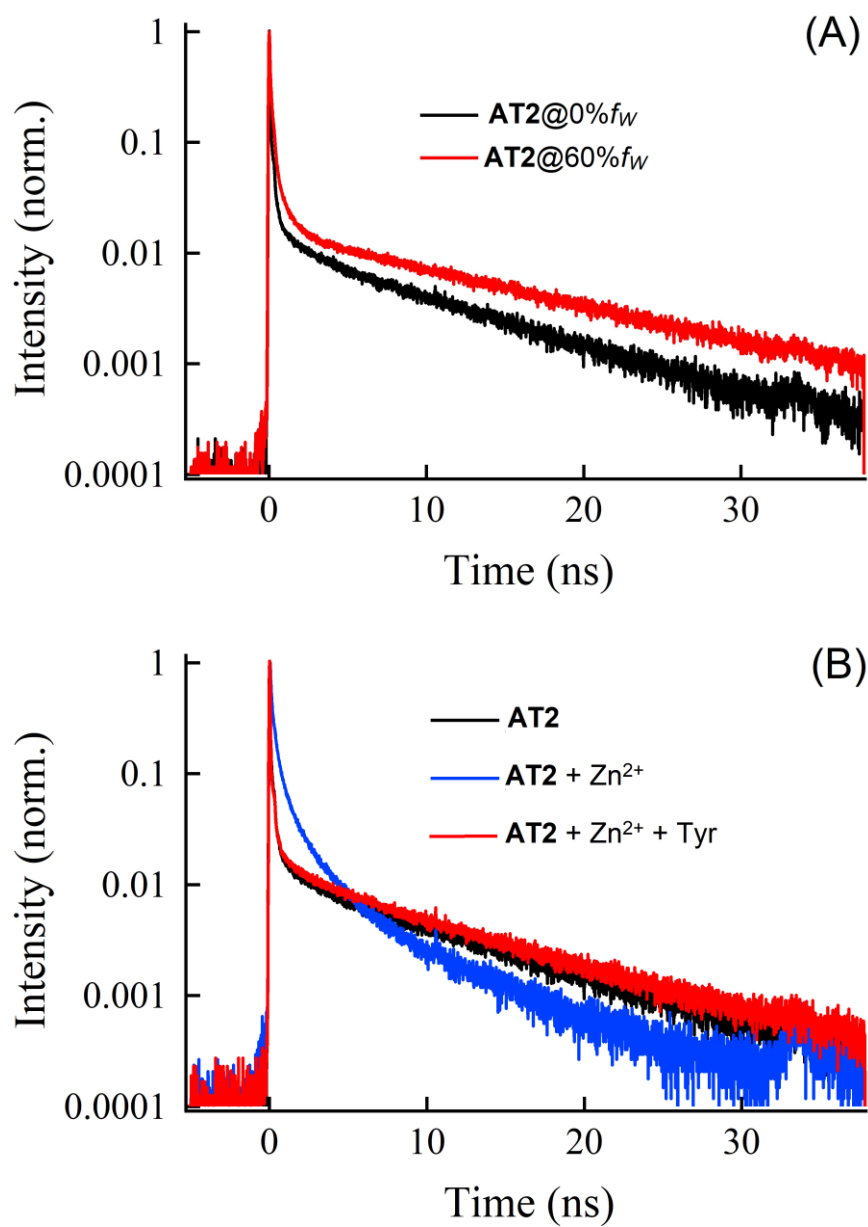


**Figure S8.** (A) TRPL spectra **AT2**@0% $f_w$  and **AT2**@60% $f_w$ ; (F) TRPL spectra of **AT2**, **AT2** +  $Zn^{2+}$ , and **AT2** +  $Zn^{2+}$  + tyrosine.

Composition	$\tau_1$ (A <sub>1</sub> )	$\tau_2$ (A <sub>2</sub> )	$\tau_3$ (A <sub>3</sub> )	$\tau_4$ (A <sub>4</sub> )	$\tau_{av}$ (ns)
AT2@0% $f_w$	0.032 (0.979)	0.502 (0.016)	9.191 (0.004)	23.982 (0.001)	0.1001
AT2@60% $f_w$	0.048 (0.933)	0.510 (0.058)	9.191 (0.006)	24.198 (0.003)	0.2021
AT2 + Zn <sup>2+</sup>	0.066 (0.800)	0.547 (0.179)	3.110 (0.020)	20.03 (0.001)	0.2329
AT2 + Zn <sup>2+</sup> + Tyr	0.031 (0.979)	0.522(0.016)	9.283 (0.004)	24.464 (0.001)	0.1003

**Table S1.** Time-resolved photoluminescence results of AT2 probe's AIEE state and its sensory complexes ( $\tau_{av} = \tau_1 * A_1 + \tau_2 * A_2 + \tau_3 * A_3 + \tau_4 * A_4$ ).

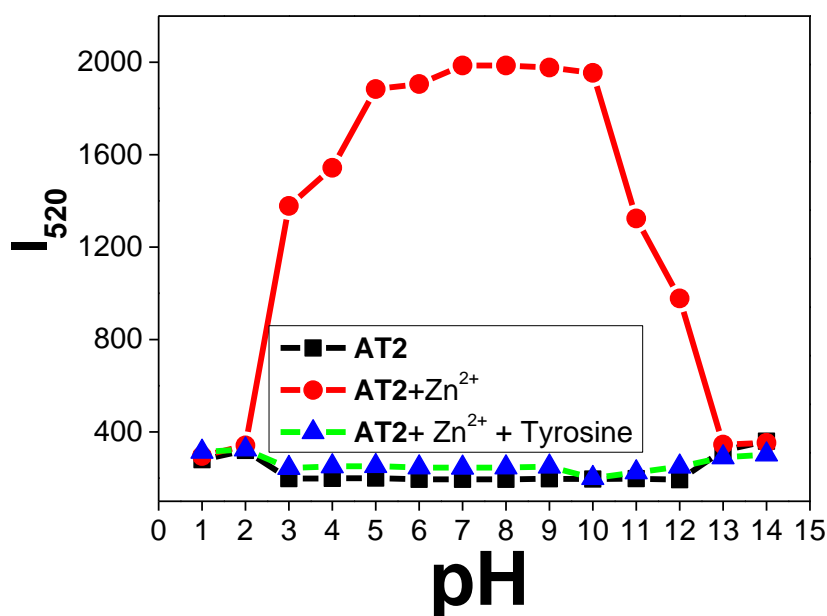


**Figure S9.** pH effect on AT2 (50  $\mu$ M in ethanol + 50  $\mu$ L 10 mM pH buffer in H<sub>2</sub>O (5%)), AT2 + Zn<sup>2+</sup> (50  $\mu$ M in ethanol + 25  $\mu$ M in H<sub>2</sub>O + 50  $\mu$ L 10 mM pH buffer in H<sub>2</sub>O (5%), separately), and AT2 + Zn<sup>2+</sup> + Tyrosine (50  $\mu$ M in ethanol + 25  $\mu$ M in H<sub>2</sub>O + 50  $\mu$ L 10 mM pH buffer in H<sub>2</sub>O (5%), individually). Note: For all pH studies, the final water percentile and volume were kept below 10% and 1 mL, respectively.

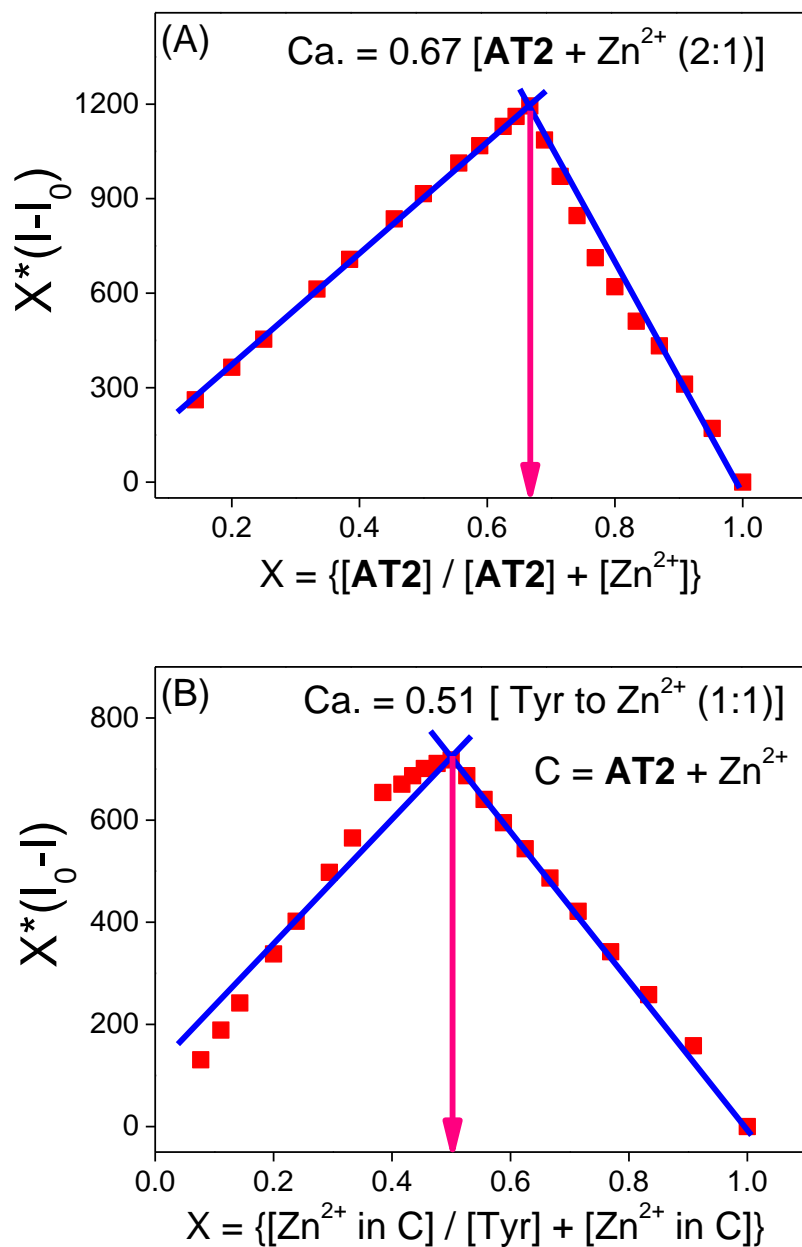


**Figure S10.** (A, B) Stoichiometry evolution from Job's plots of **AT2** + Zn<sup>2+</sup> and **AT2** + Zn<sup>2+</sup> + Tyrosine complexes representing 2:1 and 1:1 binding proportion, respectively.

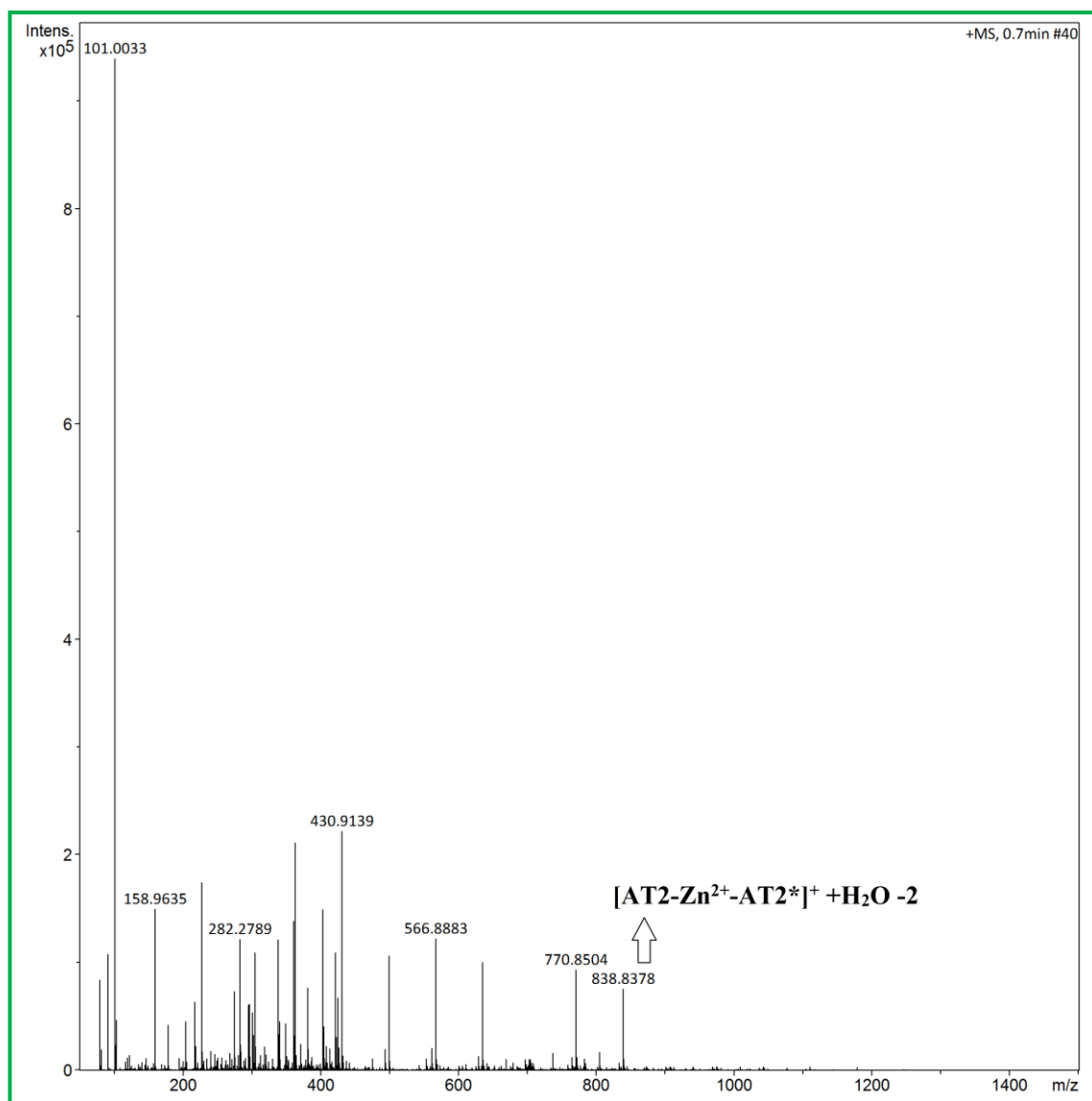


**Figure S11.** HR-Mass for AT2 + Zn<sup>2+</sup> confirming the 2:1 stoichiometric complex.

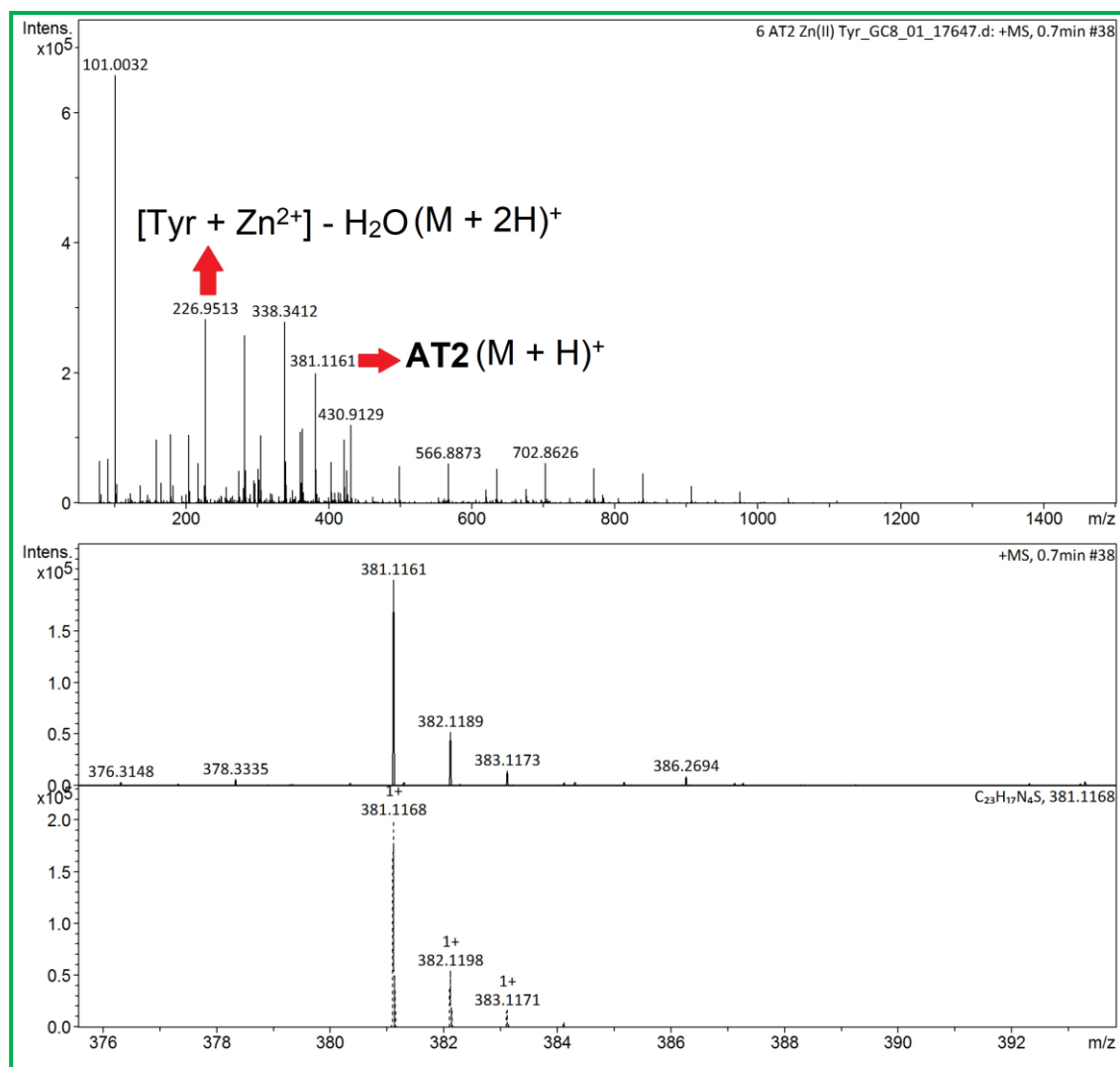


**Figure S12.** HR-Mass for **AT2** + Zn<sup>2+</sup> + Tyrosine confirming the 1:1 stoichiometric complex of Tyrosine to Zn<sup>2+</sup> ions (M + 2H)<sup>+</sup> and recovery of **AT2** probe (M + H)<sup>+</sup>.

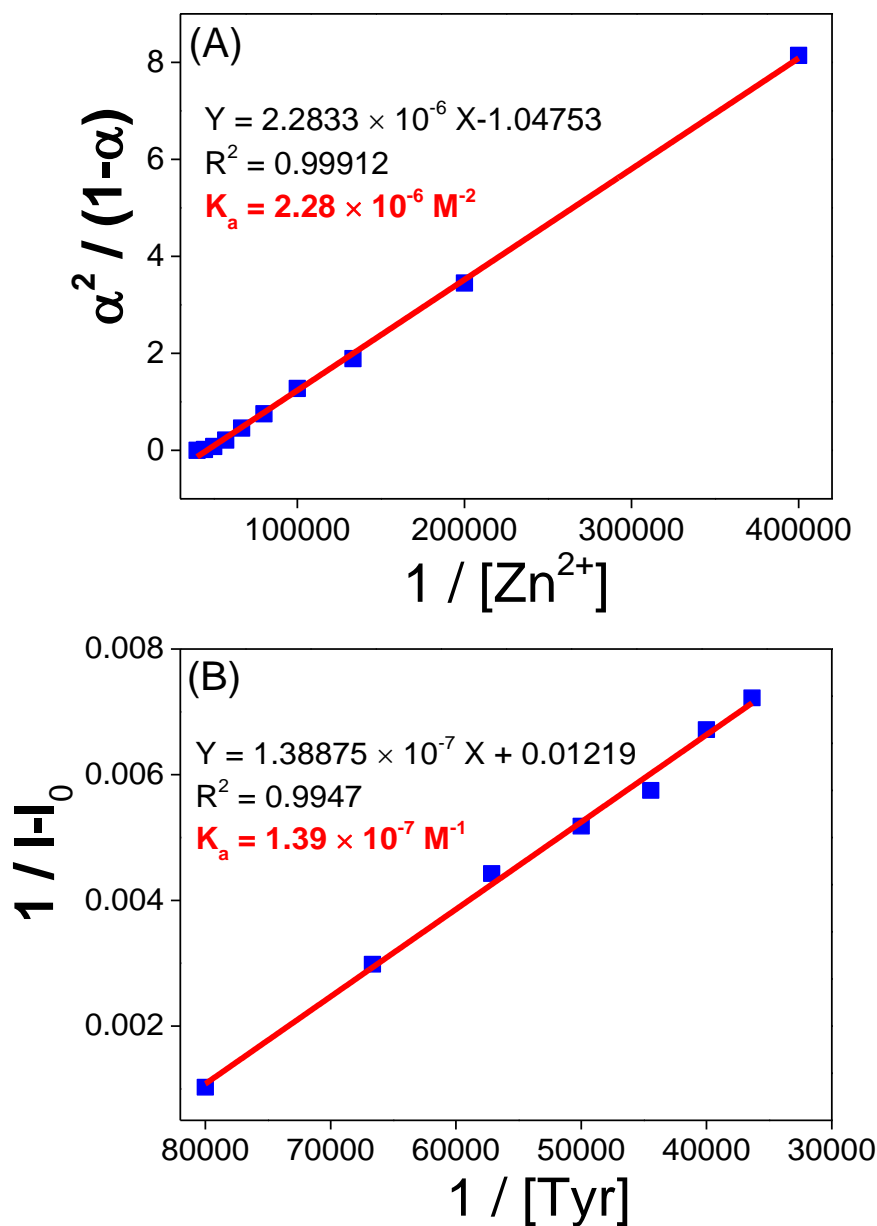


**Figure S13.** (A) Assuming 2:1 stoichiometry, the association constant of **AT2** to  $\text{Zn}^{2+}$  was evaluated by plotting  $\alpha^2/(1-\alpha)$  vs  $1/[\text{Zn}^{2+}]$ ; where  $\alpha = I-I_0/I_1-I_0$ ,  $I$  = PL intensity at 520 nm at any given  $\text{Zn}^{2+}$  concentration,  $I_0$  = PL intensity maxima in presence of  $\text{Zn}^{2+}$ , and  $I_1$  = PL intensity maxima in the absence of  $\text{Zn}^{2+}$ ; (B) Assuming 1:1 stoichiometry of Tyrosine to  $\text{Zn}^{2+}$  present in **AT2** +  $\text{Zn}^{2+}$ , the association constant was evaluated via Benesi-Hildebrand plot by plotting  $1/I-I_0$  (at 520 nm) vs  $1/[\text{Tyr}]$ ; Where  $I$  = PL intensity at 520 nm at any given Tyrosine concentration,  $I_0$  = PL Intensity in the absence of Tyrosine.

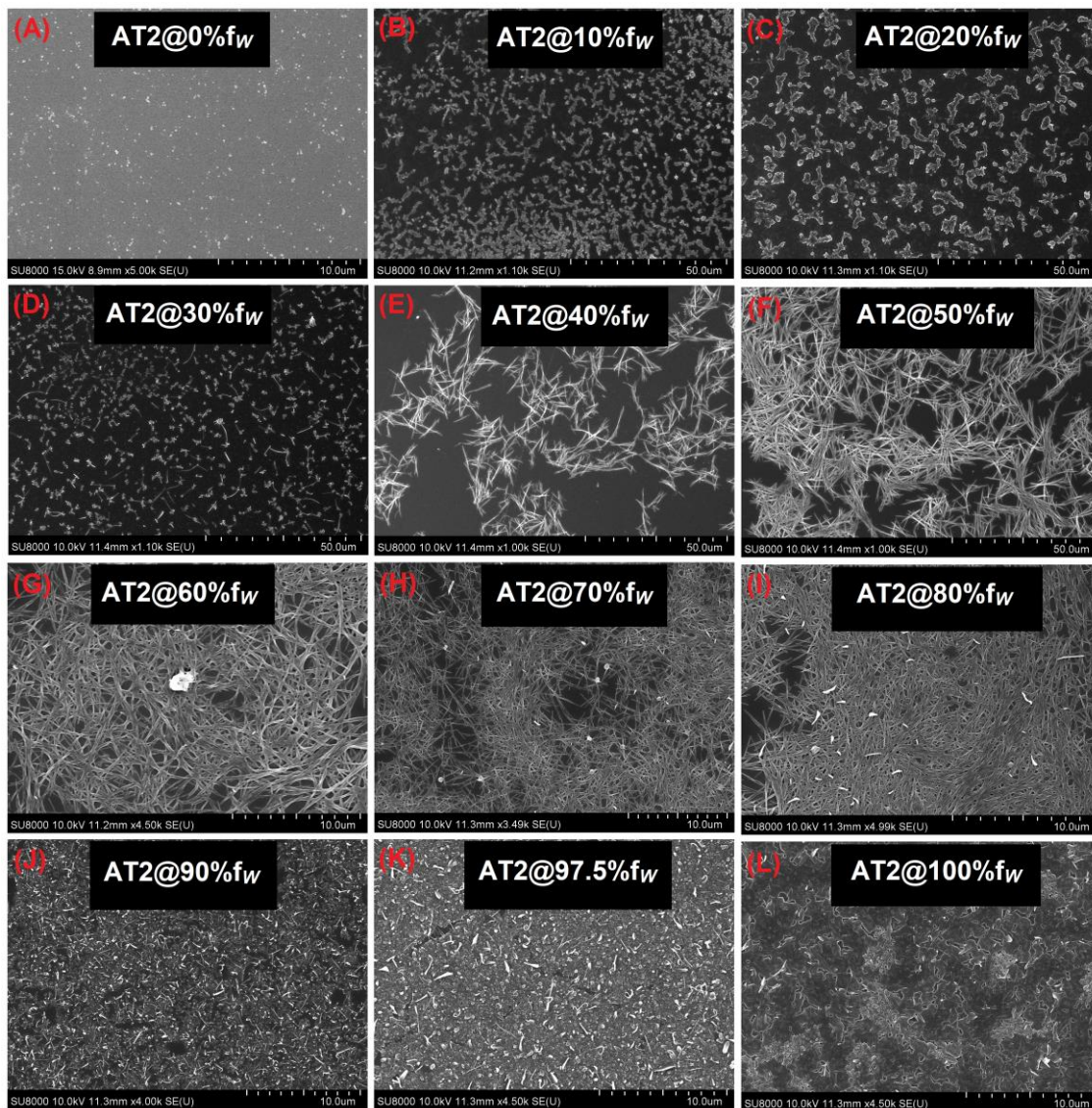


**Figure S14.** (A-L) SEM images of AT2 (50  $\mu\text{M}$  in ethanol) with increasing water fraction ( $f_w$ ) from 0 to 100%; Scale bars: images (A), (G)-(L) are at 10  $\mu\text{m}$  scale and images (B-F) are at 50  $\mu\text{m}$  scale.



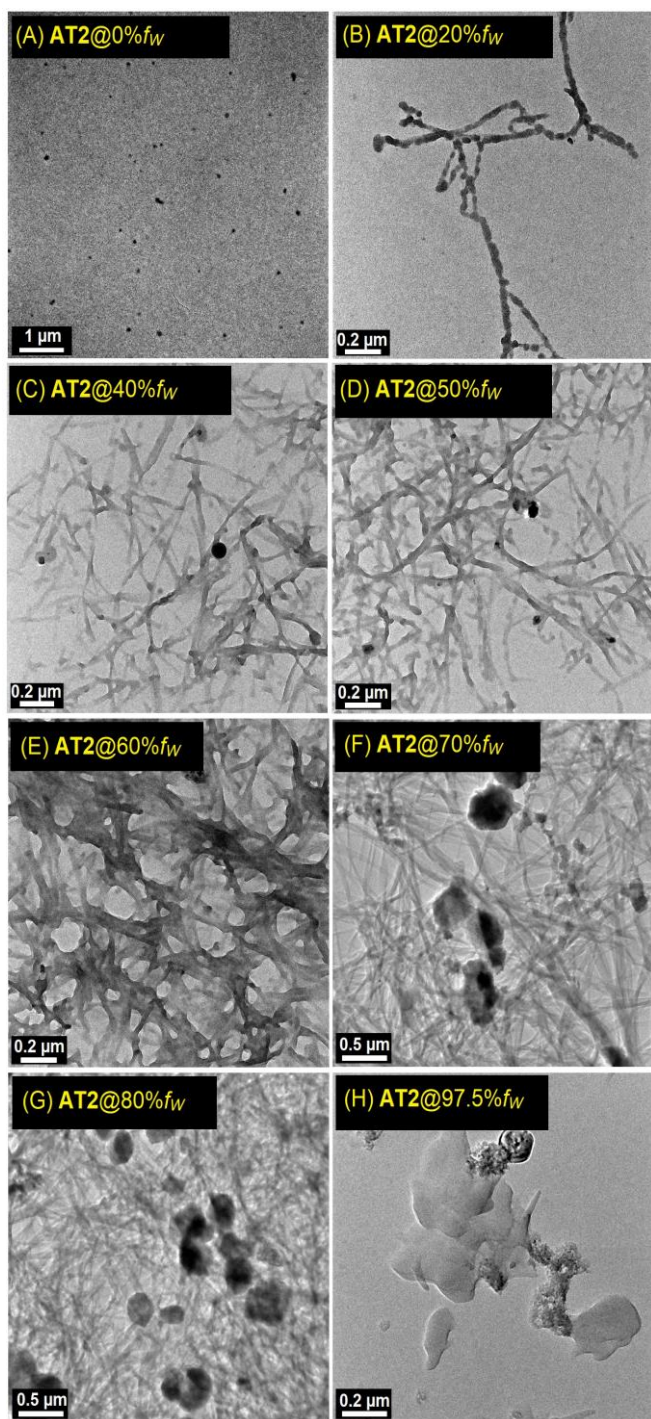


**Figure S15.** (A-H) TEM images of AT2 (50  $\mu\text{M}$  in ethanol) at water fractions ( $f_w$ ) of 0, 20, 40, 50, 60, 70, 80, and 97.5%, respectively; Scale bars: images (A) at 1  $\mu\text{m}$  scale, images (B)-(E), and (H) are at 0.2  $\mu\text{m}$  scale and images (F) and (G) are at 0.5  $\mu\text{m}$  scale.



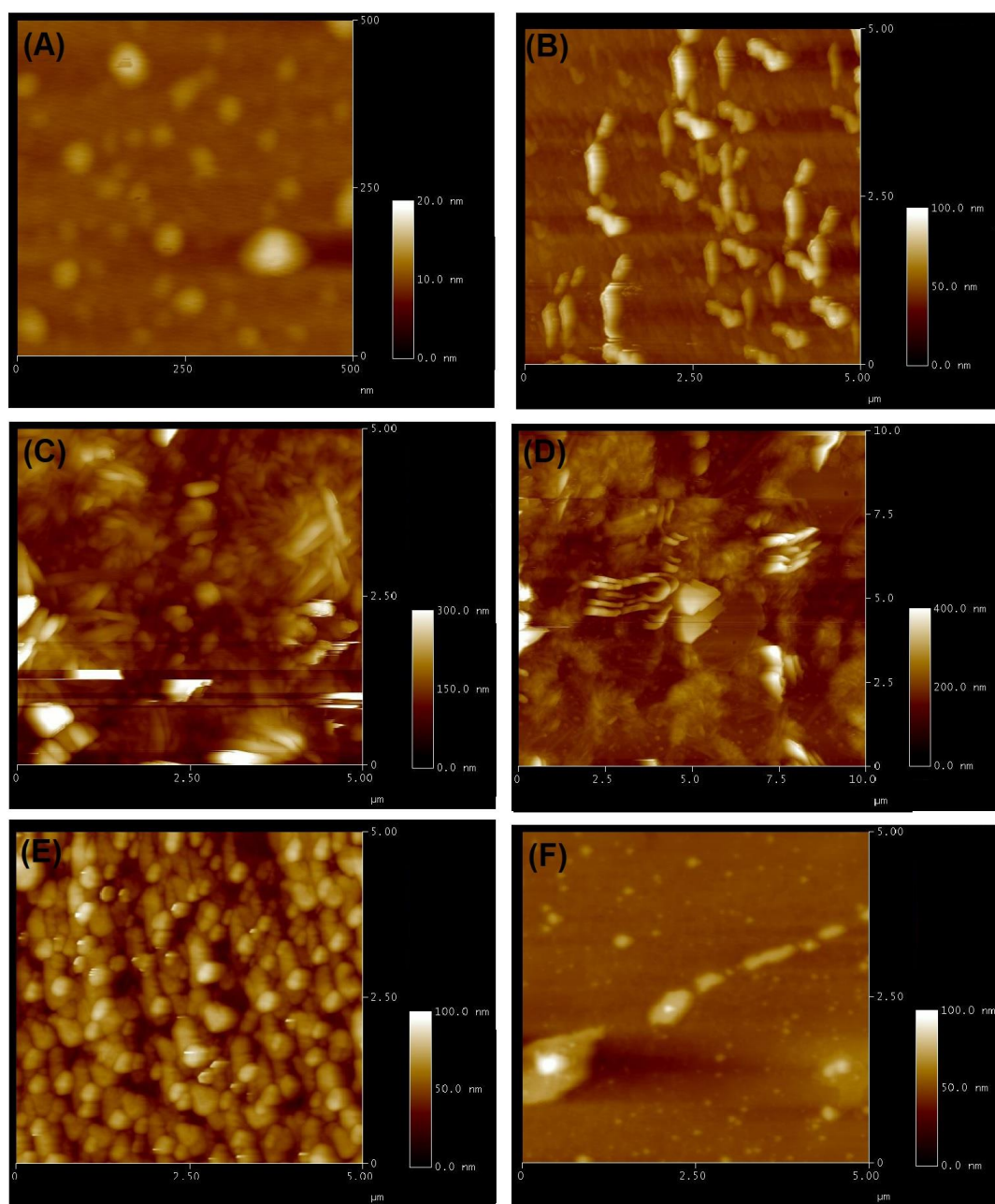


**Figure S16.** (A-D) AFM images of **AT2** (50  $\mu\text{M}$  in ethanol) at water fractions ( $f_w$ ) of 0, 30, 60, and 90%, respectively; Scale bars: (A) at 500 nm scale; (B) and (C) are at 5  $\mu\text{m}$  scale; (D) at 10  $\mu\text{m}$  scale; (E) AFM image of **AT2** +  $\text{Zn}^{2+}$  (50  $\mu\text{M}$  in ethanol + 25  $\mu\text{M}$  in  $\text{H}_2\text{O}$ ) and (F) AFM image of **AT2** +  $\text{Zn}^{2+}$  + Tyr (50  $\mu\text{M}$  in ethanol + 25  $\mu\text{M}$  in  $\text{H}_2\text{O}$  + 25  $\mu\text{M}$  in  $\text{H}_2\text{O}$ ); Scale bars: (E) and (F) are at 5  $\mu\text{m}$  scale.

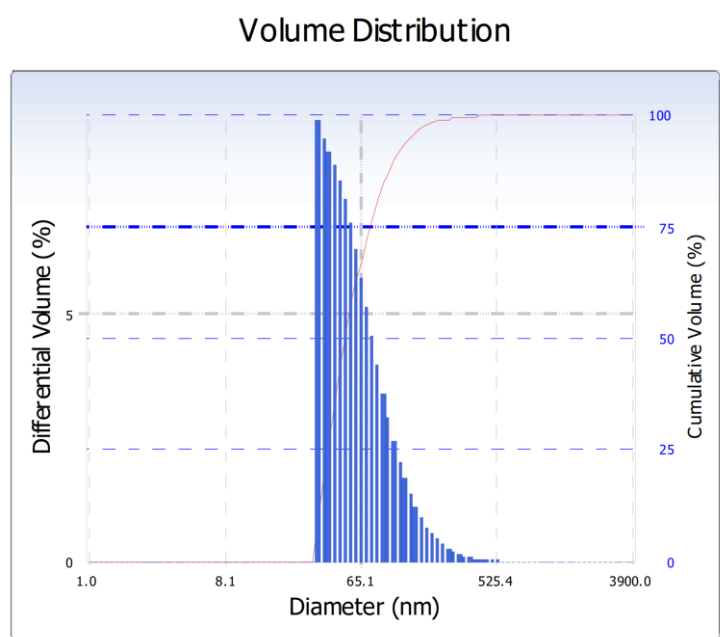


**Figure S17.** DLS of AT2 (50  $\mu$ M in ethanol) at 0% water fraction.

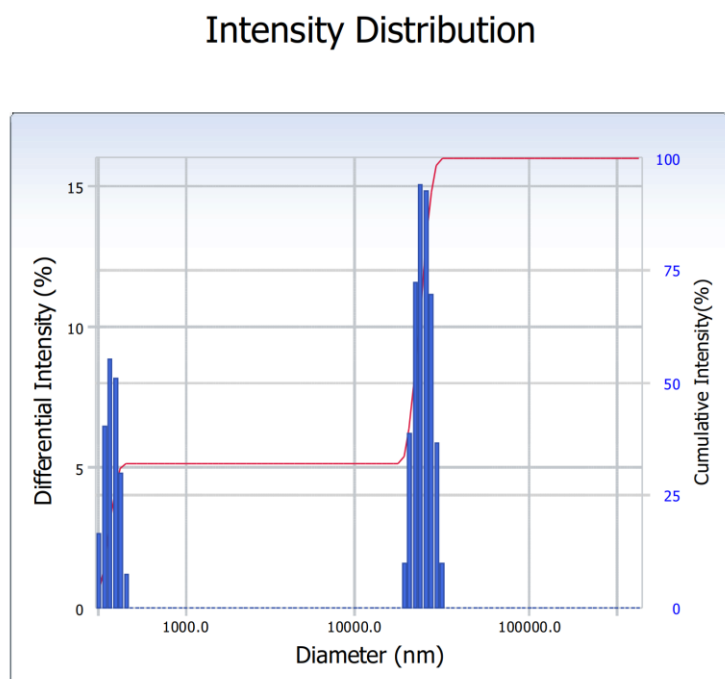


**Figure S18.** DLS of AT2 (50  $\mu$ M in  $\text{CH}_3\text{CN}$ ) at 60% water fraction.

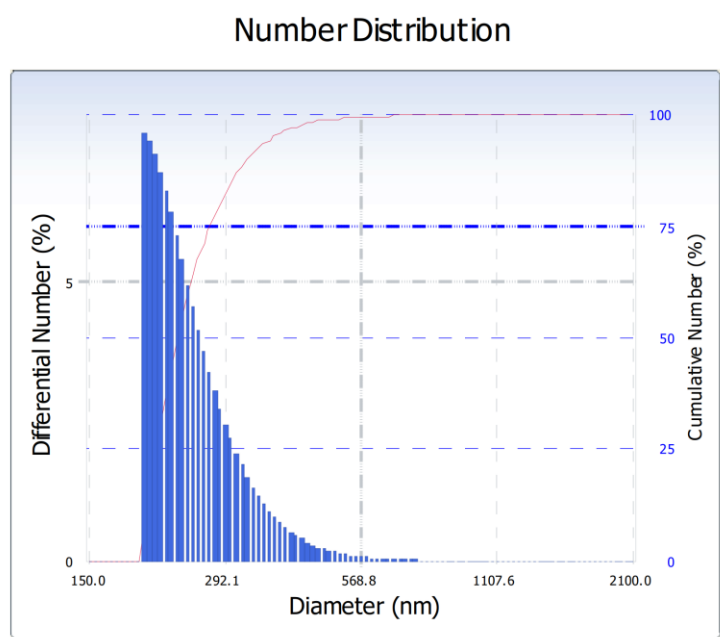


**Figure S19.** DLS of **AT2** +  $\text{Zn}^{2+}$  (**AT2**-50  $\mu\text{M}$  in ethanol +  $\text{Zn}^{2+}$ -25  $\mu\text{M}$  in water from 10 mM stock solution).

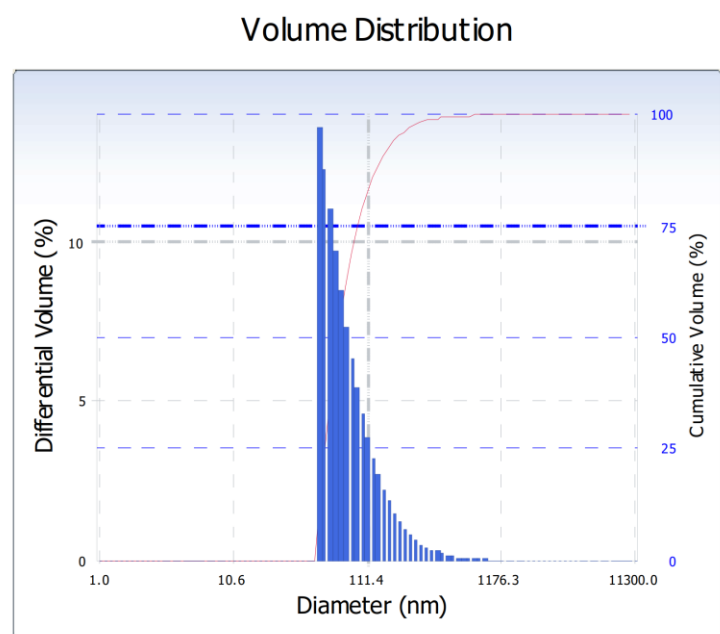


**Figure S20.** DLS of **AT2** +  $\text{Zn}^{2+}$  + Tyr (**AT2**-50  $\mu\text{M}$  in ethanol +  $\text{Zn}^{2+}$ -25  $\mu\text{M}$  in water from 10 mM stock solution + Tyrosine-25  $\mu\text{M}$  in water from 10 mM stock solution).

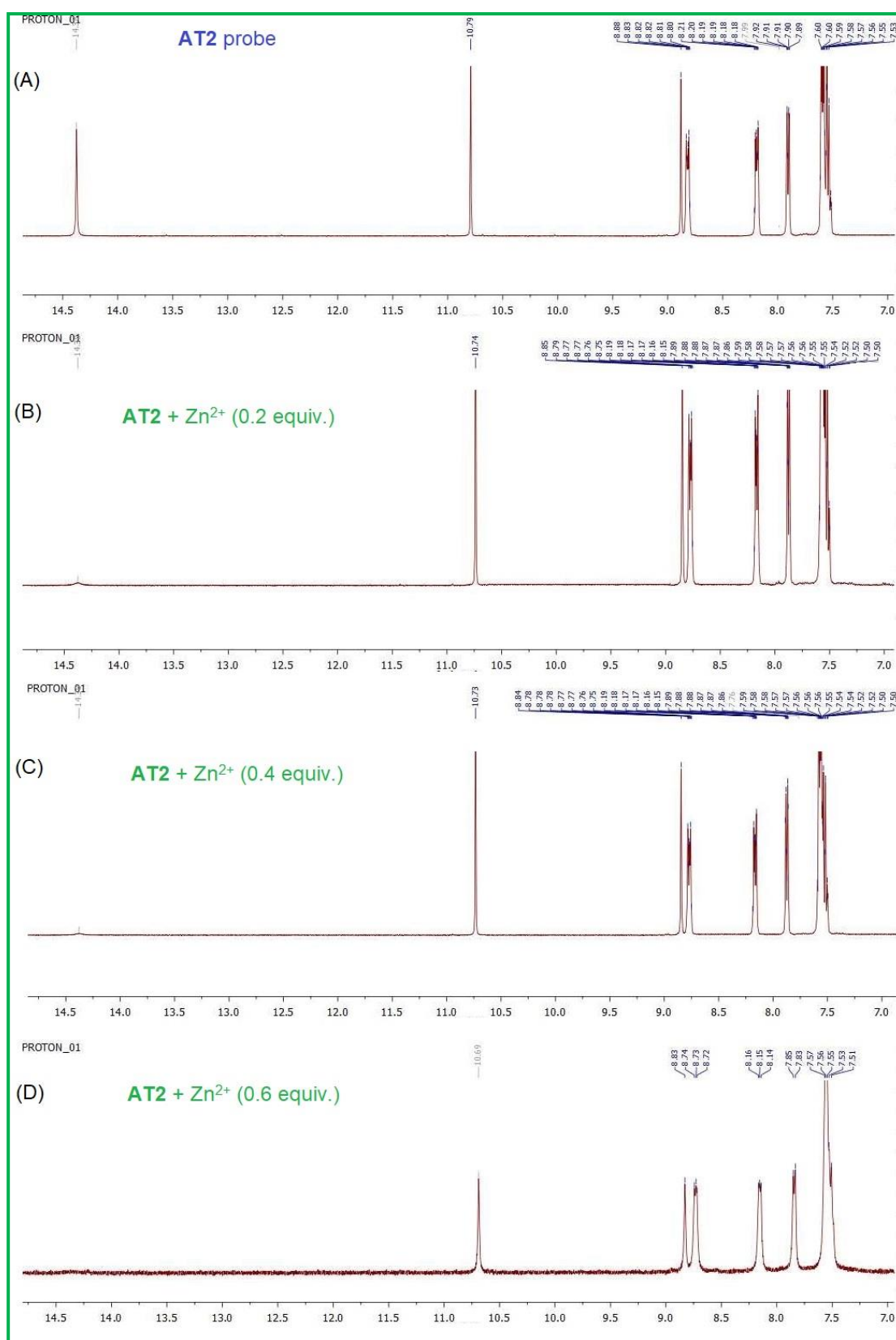


**Figure S21.** (A-D) <sup>1</sup>H NMR titration of **AT2** (20 mM in d<sub>6</sub>-DMSO) with 4, 8 and 12 mM (0.2, 0.4 and 0.6 equiv.) of Zn<sup>2+</sup> ions (from perchlorate source) in deuterated ethanol (C<sub>2</sub>D<sub>6</sub>O).

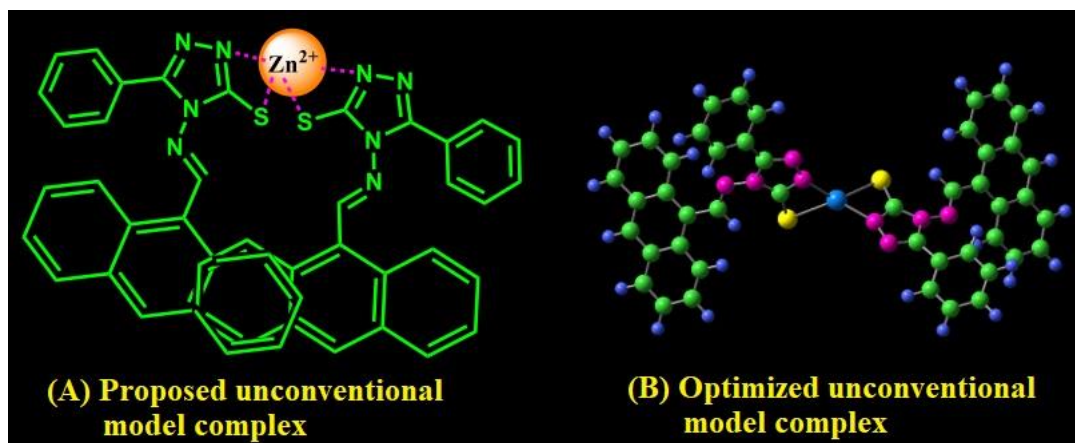


**Figure S22.** (A, B) Proposed and optimized structures of unconventional model of  $\text{AT2-Zn}^{2+}\text{-AT2}^*$ , respectively.

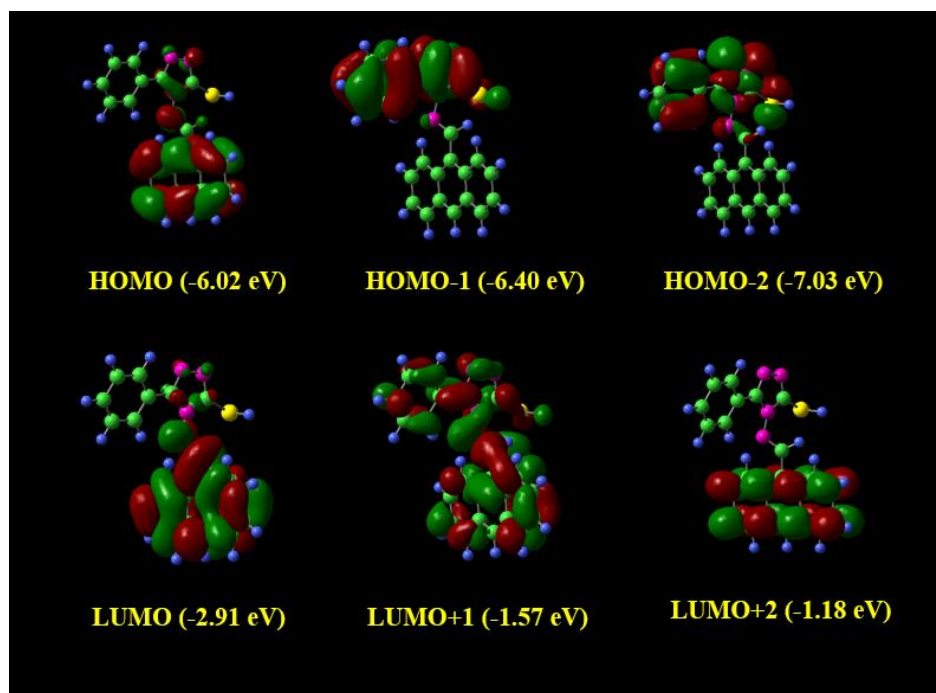


**Figure S23.** The optimized HOMOs and LUMOs of AT2-probe.

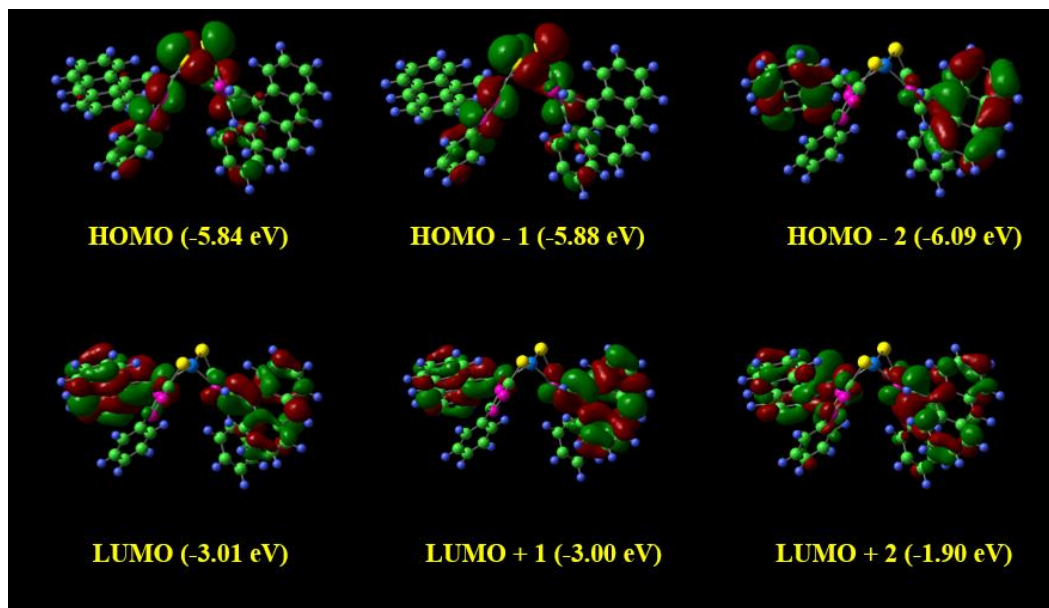


**Figure S24.** The optimized HOMOs and LUMOs of preferred complex model of  $\text{AT2-Zn}^{2+}\text{-AT2}^*$ .

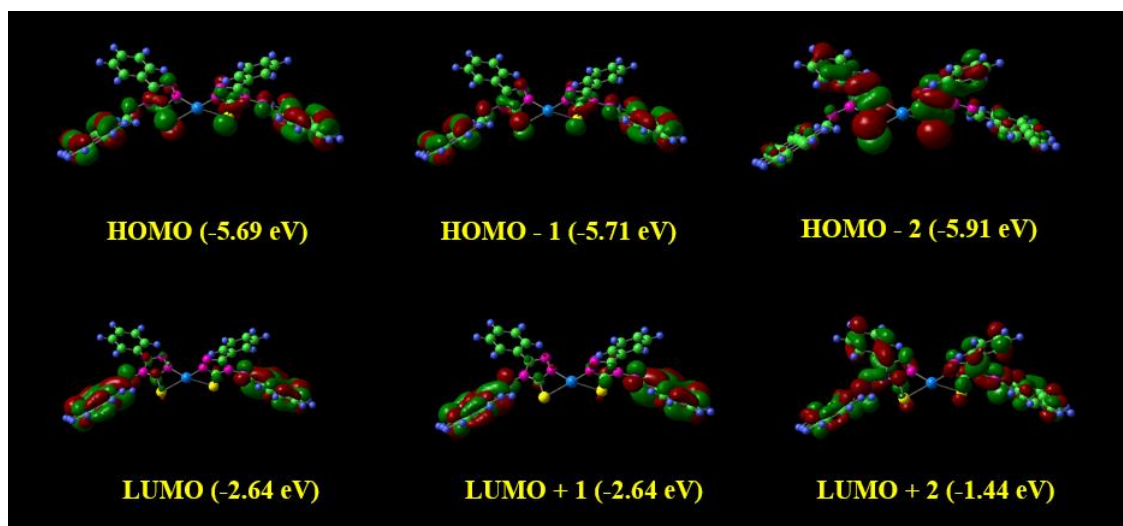


**Figure S25.** The optimized HOMOs and LUMOs of unconventional complex model of  $\text{AT2-Zn}^{2+}\text{-AT2}^*$ .



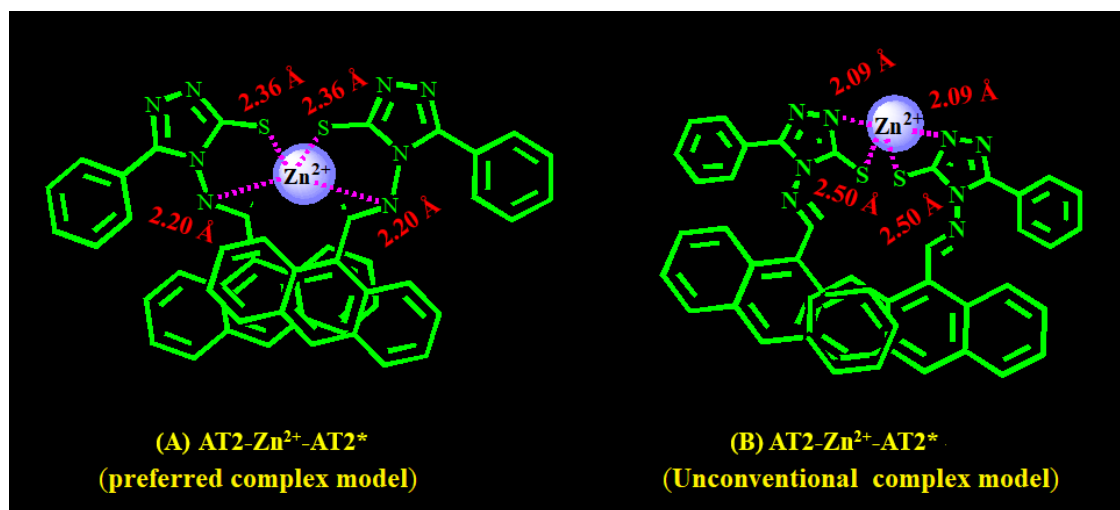


**Figure S26.** (A, B) The  $\text{Zn}^{2+}\text{---S}$  and  $\text{Zn}^{2+}\text{---N}$  bond lengths for preferred and unconventional complex models of  $\text{AT2-Zn}^{2+}\text{-AT2}^*$ .

Medium / Structure		Gas	Acetonitrile	DMSO	Ethanol
Probe	<b>AT2</b>	3.11	3.09	3.09	3.09
<b>AT2-Zn<sup>2+</sup>-AT2*</b>	Preferred complex model	2.83	2.67	2.68	2.66
	Unconventional complex model	3.05	3.08	3.08	3.09
Tyr-Zn <sup>2+</sup>		2.77 <sup>a</sup>	2.72 <sup>a</sup>	2.74 <sup>a</sup>	2.73 <sup>a</sup>

**Table S2.** The HOMOs, LUMOs and band gaps ( $E_g$ s) of **AT2** probe and  $\text{AT2-Zn}^{2+}\text{-AT2}^*$  complexes in gas, acetonitrile, DMSO and ethanol phase calculated by B3LYP/6-31+G(d,p) & LANL2DZ level of theory.

<sup>a</sup>Optimized data taken from Ref [15]

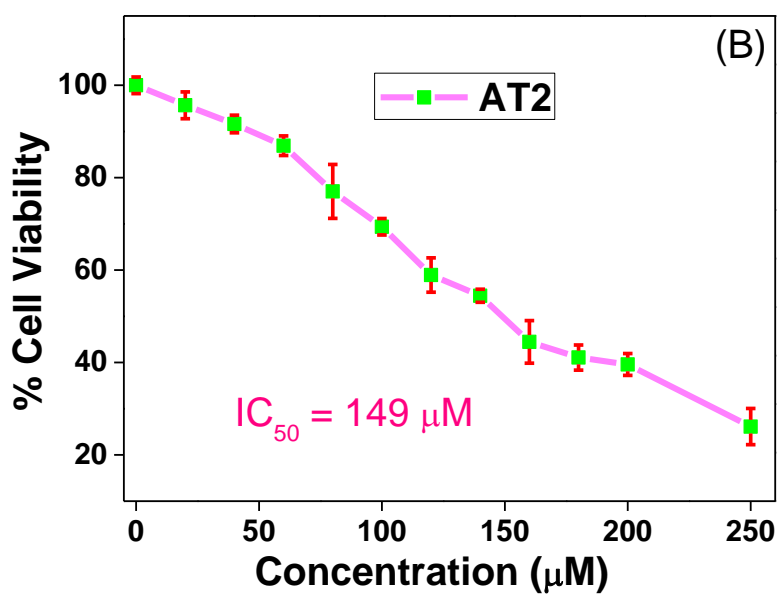
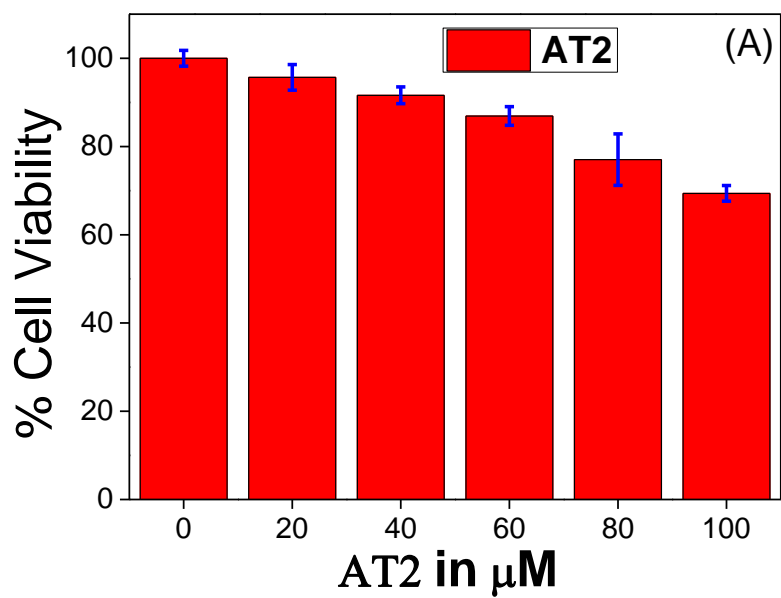


**Figure S27.** (A, B) MTT assay and  $\text{IC}_{50}$  values of **AT2** in B16-F10 cell line demonstrating its viability and biocompatibility in biological environment (n= 3).



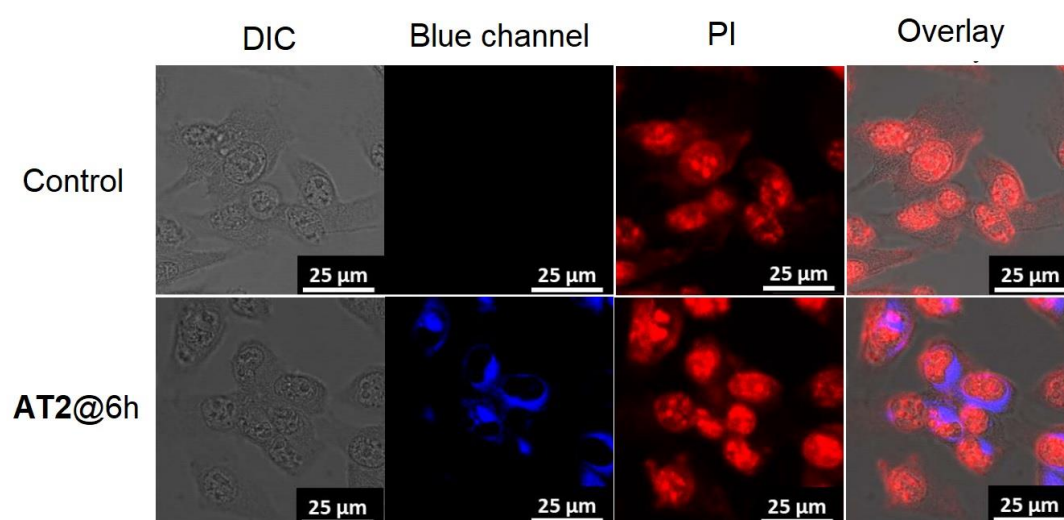


**Figure S28.** Cellular images of **AT2** after 6 hours incubation; Cell line: B16-F10; Scale bar: 25  $\mu\text{m}$ .

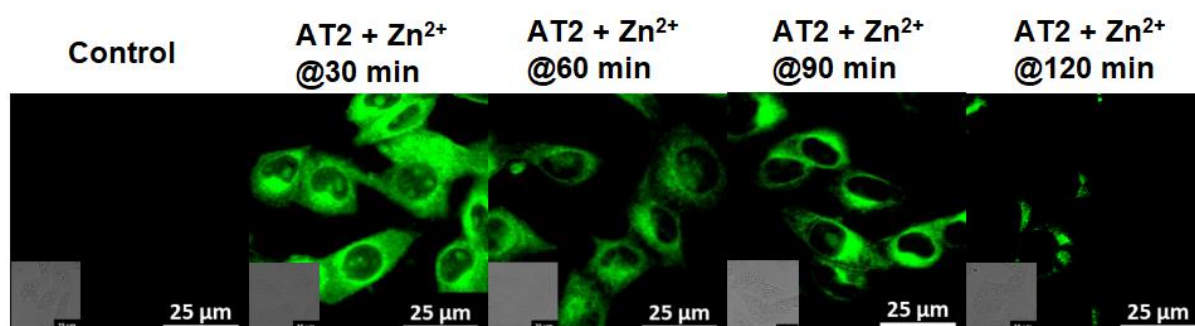


**Figure S29.** Changes in green channel cellular images of **AT2** +  $\text{Zn}^{2+}$  at 30, 60, 90, and 120 min, respectively, demonstrating the reaction between intercellular-released Tyrosine and  $\text{Zn}^{2+}$  to recover the **AT2** probe; Cell line: B16-F10; Scale bar: 25  $\mu\text{m}$ .

**Table S3.** Comparative table for Zn<sup>2+</sup> sensors by diverse probes and methods.

Probe/composition	Method	Linear range	LOD	Applications	Ref
Hydrazone probe	Fluorescent	0 – 3 $\mu$ M	66 nM	Cell imaging studies	[38]
Scorpiand macrocyclic ligand decorated with an anthracene bearing tail	Fluorescent	NA	NA	NA	[61]
1-(anthracen-9-yl)-N-(pyridin-2-ylmethyl)-N-(quinolin-2-ylmethyl)methanamine	Fluorescent	0 – 4 $\mu$ M	2.4 $\mu$ M	NA	[62]
Anthracene-based chemosensor	Fluorescent	0 – 20 $\mu$ M	36 nM	Cell imaging, and Zebra fish imaging analysis	[63]
Carbon quantum dot (CQD) from onion	Fluorescent	0 – 100 $\mu$ M	6.4 $\mu$ M	Blood plasma studies	[64]
Red-emission carbon dots-quercetin systems	Fluorescent	0.14 – 30 $\mu$ M	0.14 $\mu$ M	Real water analysis	[65]
N-(2-(bis(pyridine-2-ylmethyl)amino)ethyl)-2-mercaptoacetamide (MDPA) modified gold nanoparticles (MDPA-GNPs)	Fluorescent / SERS	1 – 120 $\mu$ M	0.32 $\mu$ M	Cell imaging studies	[66]
di-2-picolyamine (DPA)-conjugated triarylmethine (TAM) dye	Colorimetric / SERS	0-100 $\mu$ M	50 $\mu$ M	Hela cell Raman imaging studies	[67]
Coumarin based fluorescent sensors CHP and CHS	Fluorescent	0-40 $\mu$ M and 0-35 $\mu$ M	0.1 $\mu$ M and 0.19 $\mu$ M	Cell imaging studies	[68]
Anthracene -based Schiff base (4-(anthracen-9-ylmethylene) amino)-5-phenyl-4H-1,2,4-triazole-3-thiol; <b>AT2</b> )	Fluorescent	0-22.5 $\mu$ M	<b>179 nM</b>	Cell imaging, and Zebra fish imaging analysis	This work

NA = Not available

**Table S4.** Comparative table for Tyrosine sensors by diverse probes and methods.

Probe/composition	Method	Linear range	LOD	Applications	Ref
Fluorescent green carbon quantum dots (G-CQDs)	Fluorescent	2-6 $\mu\text{M}$	0.13 $\mu\text{M}$	Schottky barrier diode	[42]
Enzyme cascade-triggered colorimetric biosensor	Colorimetric	5-100 $\mu\text{M}$	2.74 nM	NA	[43]
Phosphodiesterases quaternary ammonium nanoparticles	Light Scattering	$5.5 \times 10^{-8}$ - $4.68 \times 10^{-6}$ mol/L	$1.38 \times 10^{-8}$ mol/L	Human serum and urine samples analysis	[44]
Methylene blue with urea conjugated diphenylamine group-MB1	Fluorescent	0 to 1 U/mL	NA	in-vitro and in-vivo cell imaging studies	[59]
Phenylthiourea-conjugated BODIPY photosensitizer (PTUBDP)	Fluorescent	NA	NA	in-vitro and in-vivo cell imaging studies	[60]
Graphene Oxide–Chitosan Modified Carbon-Based Electrodes	Electrochemical	1-100 $\mu\text{M}$	5.86 $\mu\text{M}$	NA	[69]
Asymmetric alumina ( $\text{Al}_2\text{O}_3$ ) nanochannels functionalized by tyramine	Electrochemical	2–50 U/mL	0.83 U/mL	Cell Lysates studies	[70]
Graphene quantum dots (GQDs)	Fluorescent	1.0–160 mmol L <sup>-1</sup>	5.0 mmol L <sup>-1</sup>	NA	[71]
Reduced graphene oxide-hemin-Ag (rGO-H-Ag) electrode	Electrochemical	0.1 to 100 $\mu\text{M}$ and 100 to 1000 $\mu\text{M}$	30 nM	Human urine sample analysis	[72]
Anthracene -based Schiff base (4-(anthracen-9-ylmethylene) amino)-5-phenyl-4H-1,2,4-triazole-3-thiol; <b>AT2</b> )	Fluorescent	0-17.5 $\mu\text{M}$	<b>667 nM</b>	Cell imaging and Zebrafish imaging analysis	This work

NA = Not available